Atomic Structure Imaging Beyond Conventional Resolution Limits in the Transmission Electron Microscope

Sarah J. Haigh,[1,*] Hidetaka Sawada,[2] and Angus I. Kirkland[1,†]

[1]*Department of Materials, University of Oxford, Parks Road, OX1 3PH, United Kingdom*

[2]*JEOL Ltd., 1-2 Musashino 3-Chome, Akishima, Tokyo 196, Japan*

(Received 5 August 2009; published 17 September 2009)

Transmission electron microscopy is an extremely powerful technique for direct characterization of local structure at the atomic scale. However, the resolution of this technique is fundamentally limited by the partial coherence of the electron beam. In this Letter we demonstrate a method that extends the ultimate resolution of the latest generation of aberration corrected transmission electron microscopes by 41% relative to that achievable using conventional axial imaging. Experimental results verify that a real space resolution of 78 pm has been achieved at 200 kV.

DOI: 10.1103/PhysRevLett.103.126101 PACS numbers: 68.37.Og, 42.30.Wb, 68.37.Lp

Transmission electron microscopy is a widely used atomic scale imaging technique and the recent development of correcting electron-optical elements [1,2] has significantly improved the attainable spatial resolution and sensitivity. However, even aberration corrected instruments are resolution limited by the partial coherence of the electron beam. Wave function restoration is a method that computationally recovers the complex wave function at the exit surface of the specimen from a multiple image data set [3–9]. While exit wave function restoration has been applied to axial aberration corrected images recorded at different defoci [10–14], the ultimate resolution is limited to that of a single axial image. In this Letter we demonstrate that the resolution of the exit wave function can be improved beyond the information limit by 41% by including aberration corrected images acquired under tilted illumination in the restoration data set. The super resolution structural information obtained by this approach will be applicable to many areas of physics, material science and nanotechnology including quantum information and catalysis where local atomic positions directly affect physical properties.

In the absence of a physical objective aperture, the partial spatial and temporal coherence of the electron beam together define an effective aperture in Fourier space, which for axial illumination is centered on the optic axis. Tilting the incident electron beam shifts this effective aperture in Fourier space, so that higher resolution information is transferred, albeit only in the direction of the beam tilt [8,15] (Fig. 1). However, if images with suitably varying illumination tilts are combined, information transfer is increased in all directions. Thus a large synthetic Fourier space aperture can be produced by combining images recorded for several illumination tilts [8,9] (see [16] for a schematic diagram illustrating this concept). This aperture synthesis approach enables data to be recovered beyond the conventional axial resolution limit and is related to techniques used in radio astronomy [17,18] and radar [19], and is the reciprocal analog of Ptychography in the scanning transmission electron microscope [20].

Experimental aperture synthesis using conventional TEM images is feasible but the uncorrected spherical aberration of the objective lens substantially limits the resolution improvement achievable [8,9]. However, using aberration corrected data significantly larger beam tilts are possible, corresponding to a greater resolution improvement [13]. This Letter outlines the first experimental results from this approach using a tilt-defocus data set geometry to provide super resolved data beyond 0.08 nm at 200 kV.

Figure 2 compares the calculated information transfer recovered in exit wave functions restored from a tilt-defocus data set [21,22] to that recovered from a focal series of images [3–7,10–14] and clearly demonstrates the recovery of super resolved information in the former. For the experimental restorations reported here images were acquired using a JEOL 2200MCO aberration corrected (S)TEM operated at 200 kV [14]. A negative 3rd order spherical aberration coefficient of $-5\ \mu$m was chosen to balance the uncorrected 5th order spherical aberration [23,24]. Axial coherent aberrations up to 5th order spherical aberration were initially measured using

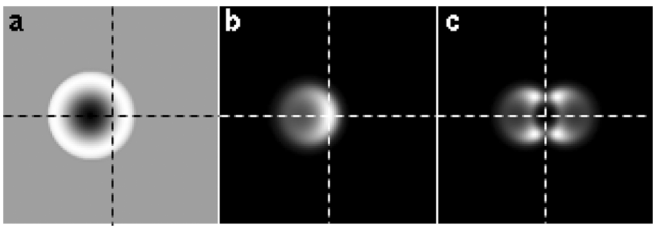

FIG. 1. (a) Phase and (b) modulus of the effective aperture for the JEOL 2200MCO TEM calculated with $-5\ \mu$m spherical aberration, Scherzer defocus, and a 16 mrad beam tilt. The corresponding diffractogram is shown in (c). The dashed cross indicates the position of the optic axis.

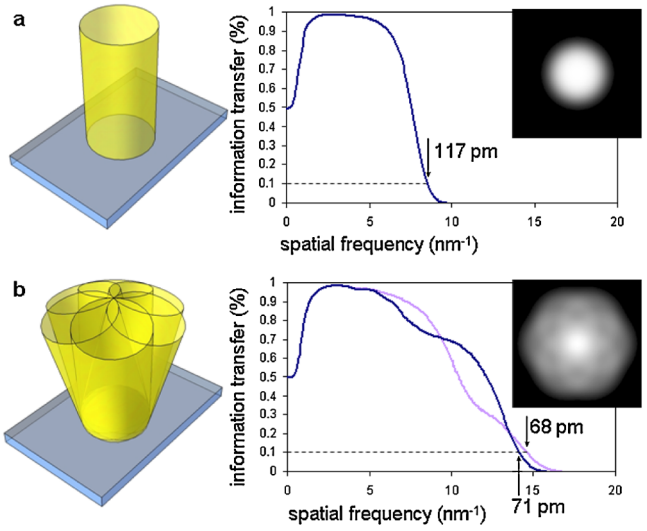

FIG. 2 (color online). Schematic diagram showing the geometry and information transfer for (a) focal series and (b) tilt series restoration with a tilt magnitude of 16 mrad. Information transfer is centrosymmetric in (a) in Fourier space (shown inset) whereas the Fourier space plot inset in (b) has a characteristic symmetry due to the use of six equally spaced illumination tilts. The bold line in (b) indicates the direction of strongest information transfer and the lighter line that of weakest information transfer. The limit where information transfer falls to below 10% is marked in both (a) and (b).

the CEOS aberration correction software [25] and for subsequent refinement were also independently remeasured from Zemlin tableaus of diffractograms obtained from a nearby region of amorphous carbon support film immediately before and after data set acquisition. The experimentally measured values of the aberration coefficients above 3rd order were computationally compensated during exit wave function restoration by using an additional Fourier space phase plate [12,26]. Focal series data sets contained 20 aberration corrected images with an average focus step of 7 nm and tilt-defocus data consisted of a three-member focal series with focal steps of 9 and 12 nm recorded at six equally spaced tilt azimuths together with additional axial images. The order of image acquisition was optimized so as to minimize hysteresis in the tilt coils and objective lens. Each image was preprocessed to eliminate the effects of the modulation transfer function for the CCD camera used [27,28] and exit wave function restoration was performed using a linear Wiener filter, with local aberrations measured using a phase compensated correlation function and phase contrast index function [21,22]. The restored exit wave functions were finally Fourier filtered to reduce residual detector noise by applying a circular mask to each reflection at a radius of 0.5 nm^{-1} with the mask edges smoothed by 0.15 nm^{-1}.

To determine the optimum illumination tilt magnitude for aperture synthetic reconstruction in an aberration corrected instrument the tilt induced changes in the wave aberration function must be considered. Limiting the phase change produced by tilt induced changes in any coherent aberration to $\pi/2$ gives a maximum tilt magnitude of 25 mrad, using the experimentally measured values of coefficients to 5th order appropriate to the instrument used. However, at these large beam tilts partial coherence in the illumination leads to a loss of transfer at the center of the tilted transfer function [8]. Limiting the extent of this loss to 50% of the highest axial transfer gives a more conservative maximum allowable tilt angle of 16 mrad. As shown in Fig. 2 the inclusion of images with this tilt magnitude in the restoration data set extends the limit at which information transfer falls below 10% to better than 71 pm (14.1 nm^{-1}) in all directions and to 68 pm (14.7 nm^{-1}) along the illumination tilt directions. In comparison, using a conventional focal series data set the equivalent limit occurs at a resolution of 117 pm (8.55 nm^{-1}).

Experimental demonstration of this resolution improvement requires a suitably thin sample, since for tilted illumination the specimen potential is projected along a different direction relative to the axial case introducing an additional phase shift. Again allowing a maximum tolerable phase shift of $\pi/2$, a simple parallax argument gives an allowable specimen thickness, $t \leq d/(2\tau)$ for a tilt magnitude, τ, and a resolution, d. For a tilt magnitude of 16 mrad this limits the specimen thickness to ~2.4 nm. Figure 3 provides a more detailed evaluation of this effect in which a full dynamical calculation using the multislice algorithm [29,30] is shown comparing axial and tilted exit wave functions for ⟨112⟩ oriented crystalline silicon. These

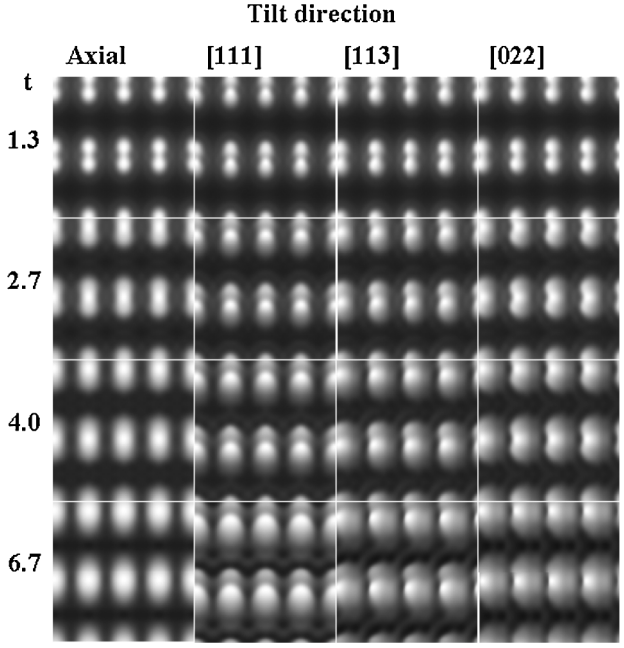

FIG. 3. Comparison of the phase of simulated exit wave functions for ⟨112⟩ oriented silicon under axial and tilted illumination for tilt magnitudes of 17 mrad in various crystallographic directions. Specimen thickness is indicated on the left-hand side in nm.

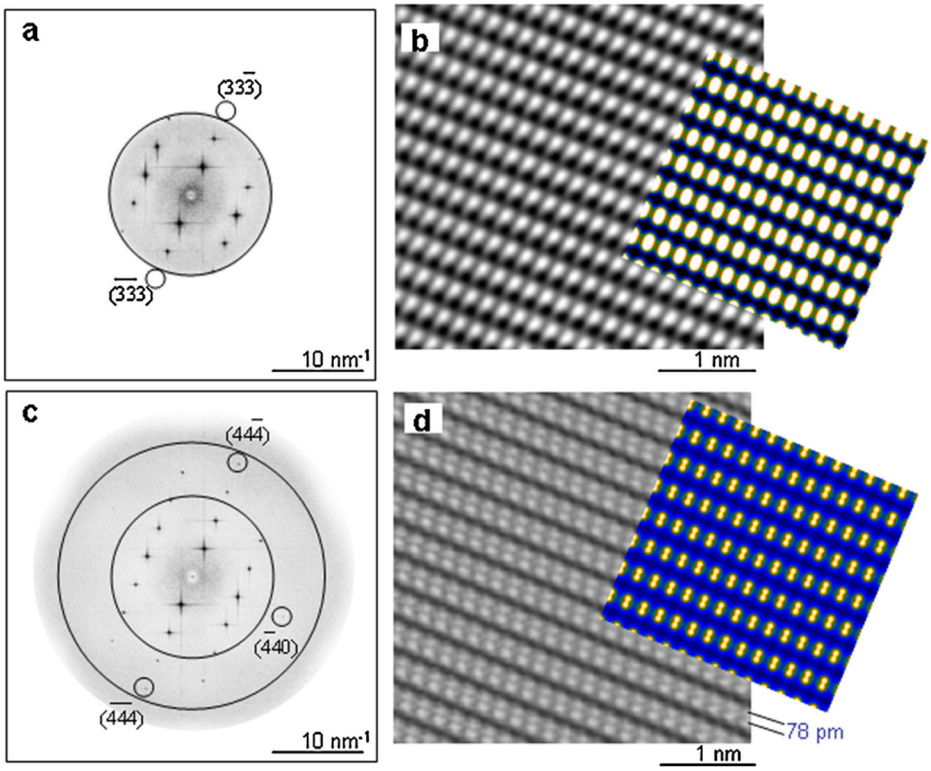

FIG. 4 (color online). Experimental restored exit wave functions for ⟨112⟩ silicon. (a) and (c) Moduli of the complex Fourier transforms of the exit wave function restored from focal and tilt-defocus series, respectively. Contrast has been inverted to improve clarity with a 10% information limit corresponding to a real space resolution of 0.117 nm indicated. In (c) the 10% information limit for the tilt-defocus data set in the direction of weakest transfer (corresponding to 0.071 nm resolution) is also indicated. (b) and (d) Subregions of the phase of the specimen exit wave function restored from focal series and from the tilt-defocus data set, respectively, with simulated wave functions overlaid.

are found to be at least qualitatively similar for a 17 mrad tilt magnitude in any direction up to sample thicknesses of 4–5 nm. Changes with respect to the axial wave function are greatest in tilt directions perpendicular to the {444} reflections corresponding to the smallest resolvable distance.

This improved transfer is experimentally demonstrated in Fig. 4 for silicon oriented along a ⟨112⟩ direction. Figures 4(a) and 4(c) show the modulus of the complex Fourier transform of the exit wave functions restored using the experimental conditions used to generate Fig. 2. Some examples of the raw images used in the restoration can be seen in Ref. [16]. Using a focal series of images the highest spatial frequency transferred corresponds to the {333} reflections which are restored with 2% transfer [Fig. 4(a)]. For comparison using a tilt-defocus data set [Fig. 4(c)] both {333} and {444} reflections are visible even at the thinnest sample regions and are recovered at a level greater than twice the background noise. In the thicker region of the specimen the first extinction distance of the {444} reflections is observed indicating that the area of the specimen shown in Figs. 4(b) and 4(d) has a thickness less than 4.7 nm. The appearance of the kinematically forbidden {222} reflections in the Fourier transforms in Fig. 4 is likely to be due to multiple scattering in the thickest regions of the ~1200 nm^2 field of view.

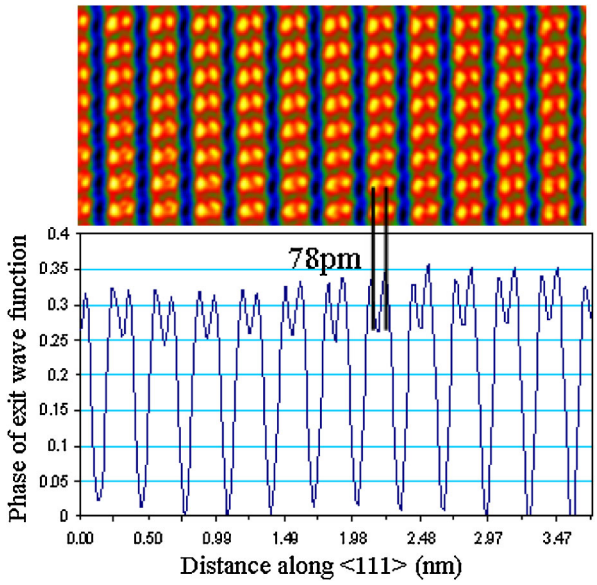

FIG. 5 (color online). Enlarged region of the phase of the silicon ⟨112⟩ exit wave function restored from a tilt-defocus series shown in Fig. 4(d), false colored to improve visibility. The lower part of the figure shows a line scan with a width of 5 pixels along ⟨111⟩ passing though the lowest row of atoms and shows a contrast dip between atom positions of 22%–26% of the peak height.

Figures 4(b) and 4(d) show the phase of the exit wave function restored from focal and tilt-defocus data, respectively. The 78 pm atomic separation (arising from the inclusion of the {444} reflections) is not recovered using focal series data and consequently the two atoms' positions appear unresolved as a single peak in projection [Fig. 4(b)]. However, when tilted illumination images are included in the restoration this reflection is strongly transferred and the atom positions are clearly resolved, with contrast dips between the peaks at the atomic positions ranging from 22% to 26% of the maximum peak height (Fig. 5).

We have shown for the first time that the inclusion of tilted illumination aberration corrected images in data sets for specimen exit wave function restoration can increase continuous information transfer to 71 pm at 200 kV, an improvement of 41% over the conventional axial limit for the microscope used. This method provides super resolved data beyond that achievable using conventional axial imaging and is moreover applicable to the latest generation of corrected instrumentation [31,32] suggesting that an ultimate target resolution of 30 pm is achievable.

This work was supported by EPSRC under grant EP/F048009/1. We also acknowledge JEOL Ltd. for providing technical assistance and financial support.

*sarah.haigh@materials.ox.ac.uk
†angus.kirkland@materials.ox.ac.uk

[1] M. Haider, S. Uhlemann, E. Schwan, H. Rose, B. Kabius, and K. Urban, Nature (London) **392**, 768 (1998).
[2] M. Haider, H. Rose, S. Uhlemann, E. Schwan, B. Kabius, and K. Urban, Ultramicroscopy **75**, 53 (1998).
[3] P. Schiske, in *Proceedings of the 4th European Regional Congress on Electron Microscopy* (Tipografia Poliglotta Vaticana, Rome, Italy, 1968), Vol. 1, p. 145.
[4] D. van Dyck, M.Op de Beeck, and W. Coene, Optik **93**, 103 (1993).
[5] W. Coene, G. Janssen, M. Op de Beeck, and D. van Dyck, Phys. Rev. Lett. **69**, 3743 (1992).
[6] W. M. J. Coene, A. Thust, M. Op de Beeck, and D. van Dyck, Ultramicroscopy **64**, 109 (1996).
[7] H. W. Zandbergen and D. van Dyck, Solid State Ionics **131**, 35 (2000).
[8] A. Kirkland, W. Saxton, K.-L. Chau, K. Tsuno, and M. Kawasaki, Ultramicroscopy **57**, 355 (1995).
[9] A. I. Kirkland, W. O. Saxton, and G. Chand, J. Electron Microsc. **46**, 11 (1997).
[10] K. Tillmann, A. Thust, and K. Urban, Microsc. Microanal. **10**, 185 (2004).
[11] L. Y. Chang, C. Maunders, E. A. Baranova, C. Bock, and G. A. Botton, Microsc. Microanal. **14**, 426 (2008).
[12] L. C. Gontard, L. Y. Chang, C. J. D. Hetherington, A. I. Kirkland, D. Ozkaya, and R. E. Dunin-Borkowski, Angew. Chem., Int. Ed. **46**, 3683 (2007).
[13] C. J. D. Hetherington, L. Y. S. Chang, S. Haigh, P. D. Nellist, L. C. Gontard, R. E. Dunin-Borkowski, and A. I. Kirkland, Microsc. Microanal. **14**, 60 (2008).
[14] J. L. Hutchison, J. M. Titchmarsh, D. J. H. Cockayne, R. C. Doole, C. J. D. Hetherington, A. I. Kirkland, and H. Sawada, Ultramicroscopy **103**, 7 (2005).
[15] More accurately, the temporal coherence envelope is wider under tilted illumination than under axial illumination, and hence the effective aperture covers a larger area than that predicted from a simple aperture shift in Fourier space.
[16] See EPAPS Document No. E-PRLTAO-103-054939 for supplementary material. For more information on EPAPS, see http://www.aip.org/pubservs/epaps.html.
[17] M. Ryle and D. Vonberg, Nature (London) **158**, 339 (1946).
[18] M. Ryle, Nature (London) **239**, 435 (1972).
[19] E. D. R. Shearman and J. Clarke, Nature (London) **219**, 143 (1968).
[20] P. D. Nellist, B. C. McCallum, and J. M. Rodenburg, Nature (London) **374**, 630 (1995).
[21] R. R. Meyer, A. I. Kirkland, and W. O. Saxton, Ultramicroscopy **92**, 89 (2002).
[22] R. R. Meyer, A. I. Kirkland, and W. O. Saxton, Ultramicroscopy **99**, 115 (2004).
[23] M. Lentzen, B. Jahnen, C. L. Jia, A. Thust, K. Tillmann, and K. Urban, Ultramicroscopy **92**, 233 (2002).
[24] L. Y. Chang, A. I. Kirkland, and J. M. Titchmarsh, Ultramicroscopy **106**, 301 (2006).
[25] S. Uhlemann and M. Haider, Ultramicroscopy **72**, 109 (1998).
[26] A. Kirkland, R. Meyer, and L. Chang, Microsc. Microanal. **12**, 461 (2006).
[27] R. R. Meyer, A. I. Kirkland, R. E. Dunin-Borkowski, and J. L. Hutchison, Ultramicroscopy **85**, 9 (2000).
[28] R. R. Meyer and A. I. Kirkland, Microsc. Res. Tech. **49**, 269 (2000).
[29] J. M. Cowley and A. F. Moodie, Acta Crystallogr. **10**, 609 (1957).
[30] P. Goodman and A. F. Moodie, Acta Cryst. A **30**, 280 (1974).
[31] C. Kisielowski, B. Freitag, M. Bischoff, H. van Lin, S. Lazar, G. Knippels, P. Tiemeijer, M. van der Stam, S. von Harrach, and M. Stekelenburg, Microsc. Microanal. **14**, 469 (2008).
[32] H. Sawada, Y. Tanishiro, N. Ohashi, T. Tomita, F. Hosokawa, T. Kaneyama, Y. Kondo, and K. Takayanagi, J. Electron Microsc. (to be published).